# Supporting Information

## "*Turn-On*" fluorescent chemosensor for Zinc (II) dipodal ratiometric receptor: Application in live cell imaging.

**Kundan Tayade [a,b], Banashree Bondhopadhyay[d] Hemant Sharma[c], Anupam Basu[d], Vikas Gite[a], Sanjay Attarde[b], Narinder Singh*[c], Anil Kuwar*[a]**

[a]School of Chemical Sciences, North Maharashtra University, Jalgaon 425 001 (MS) India.

[b]School of Environmental and Earth Sciences, North Maharashtra University, Jalgaon 425 001 (MS) India.

[c]Department of Chemistry, Indian Institute of Technology, Ropar, Rupanagar (Punjab) India.

[d]Molecular Biology and Human Genetics Laboratory, Department of Zoology, The University of Burdwan, Burdwan, West Bengal, India.

---

*** Corresponding authors**. Tel.: +91-257-2257432; fax: +91-257-2257403

E-mail addresses: kuwaras@gmail.com
nsingh@iitrpr.ac.in

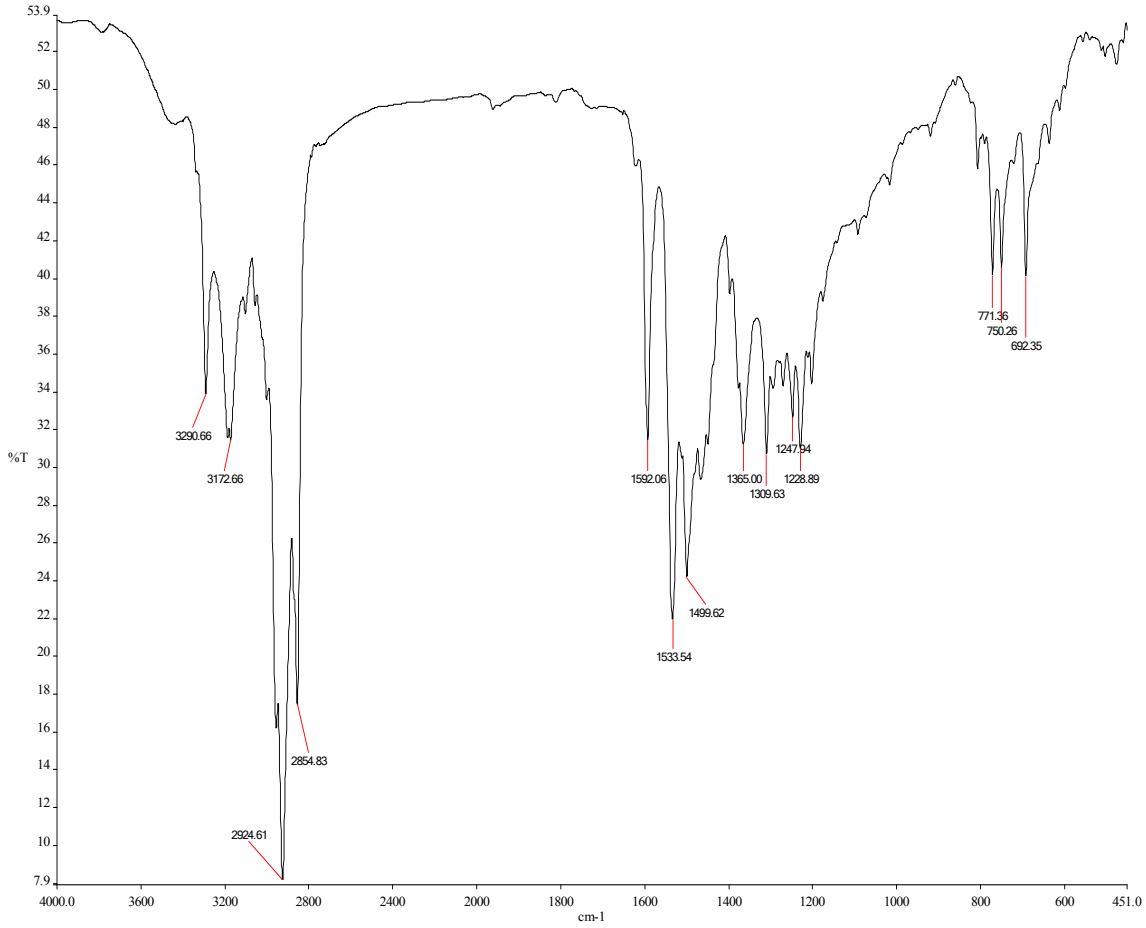


**Figure S1.** IR spectra of receptor **2**

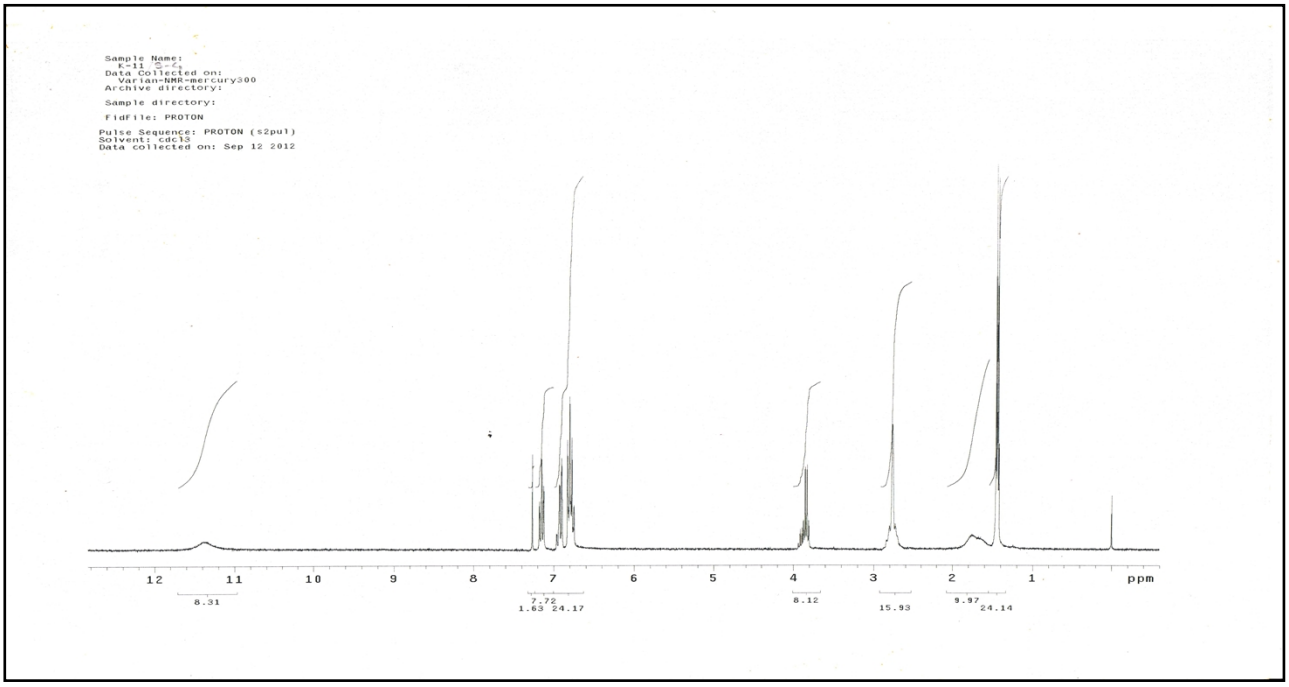

**Figure S2.** [1]H-NMR spectra of receptor **2**

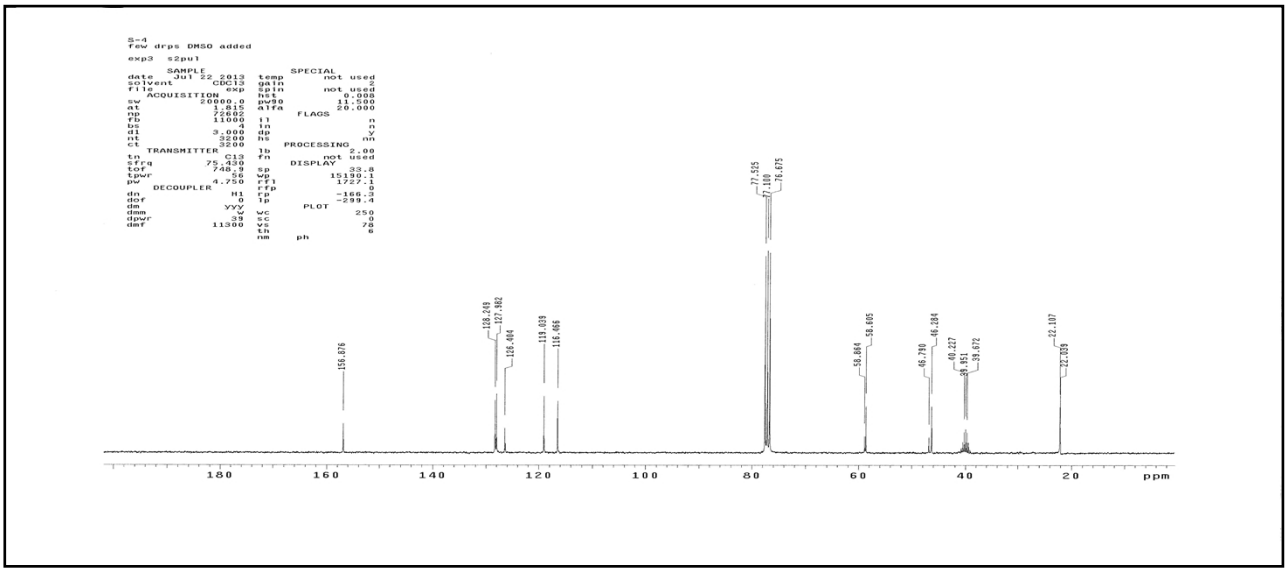

**Figure S3.** [13]C-NMR spectra of receptor **2**

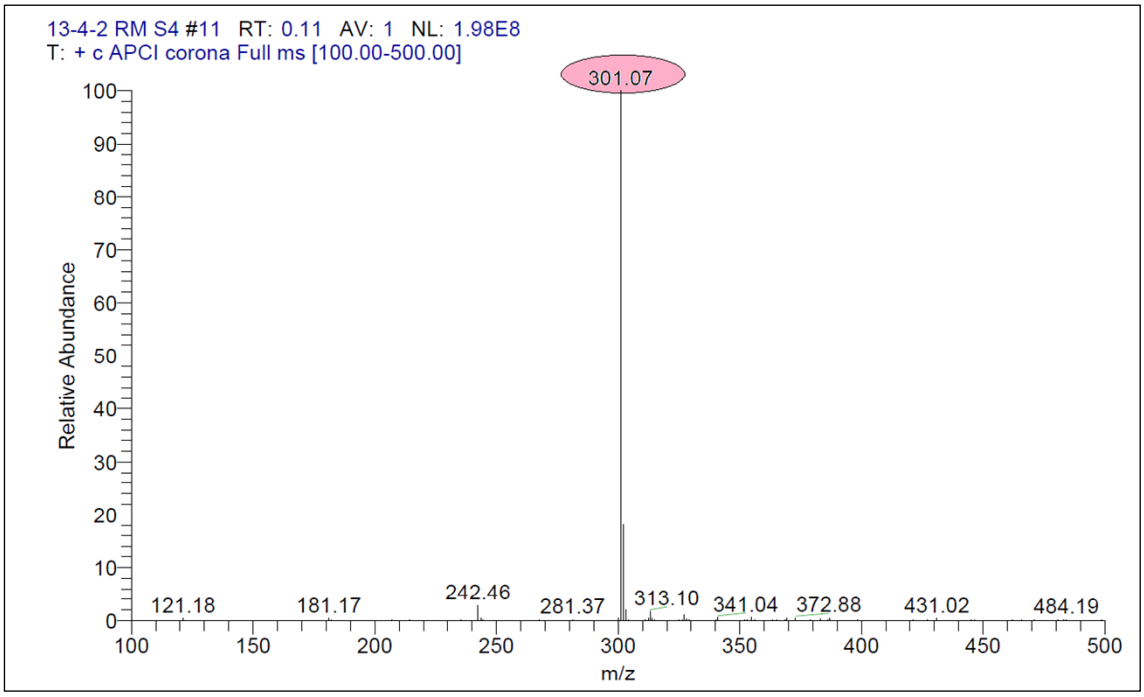


**Figure S4.** LC-MS spectra of receptor **2 (M+H$^+$)**

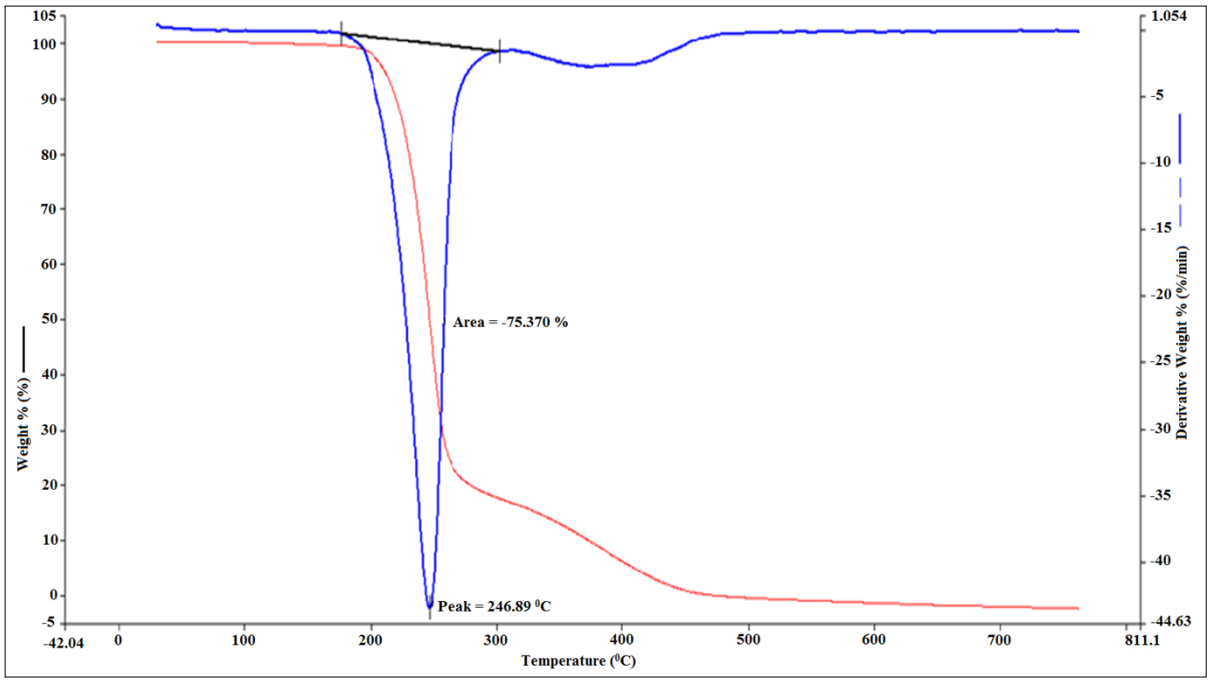


**Figure S5a.** TGA of receptor **2** (heating rate 10 ℃ per minute under nitrogen environment).

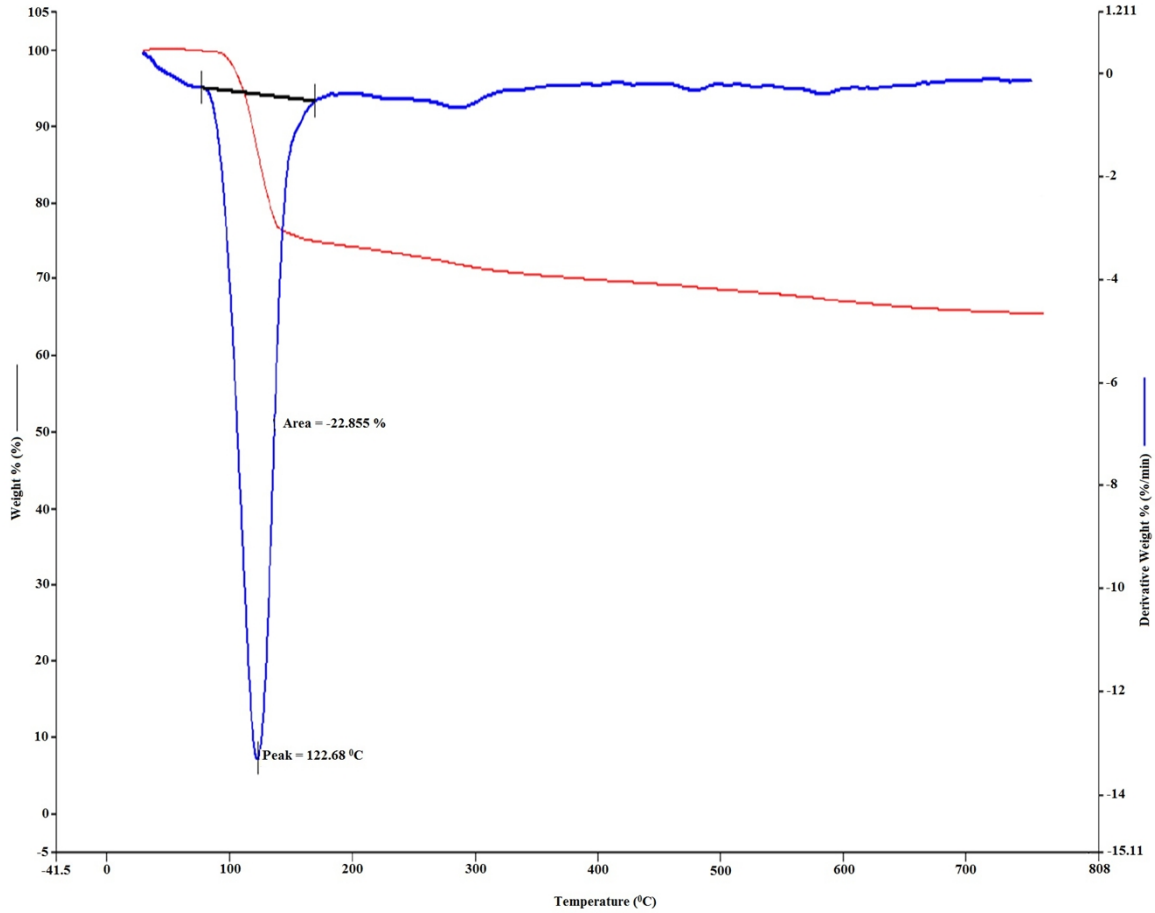


**Figure S5b.** TGA of receptor **2**.$Zn^{2+}$ (heating rate 10 ℃ per minute under nitrogen environment).

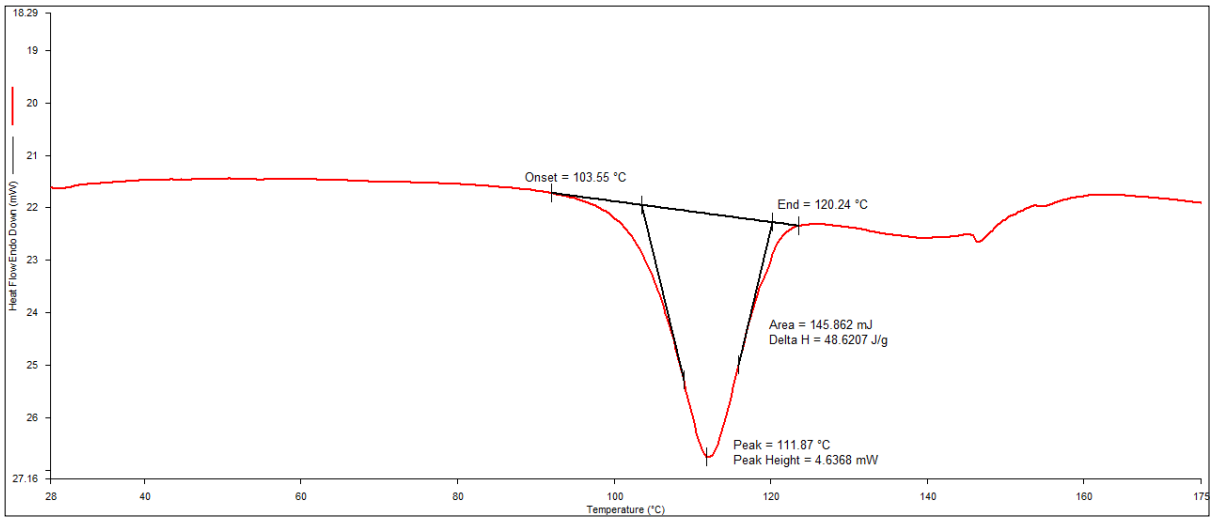


**Figure S6a.** DSC of receptor **2**.

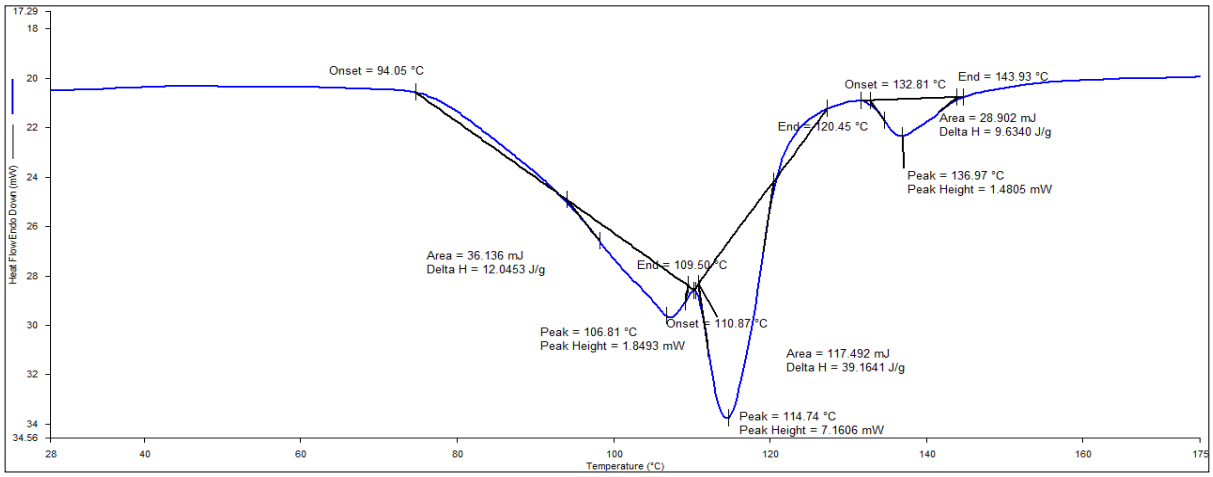


**Figure S6b.** DSC of receptor **2**.$Zn^{2+}$.

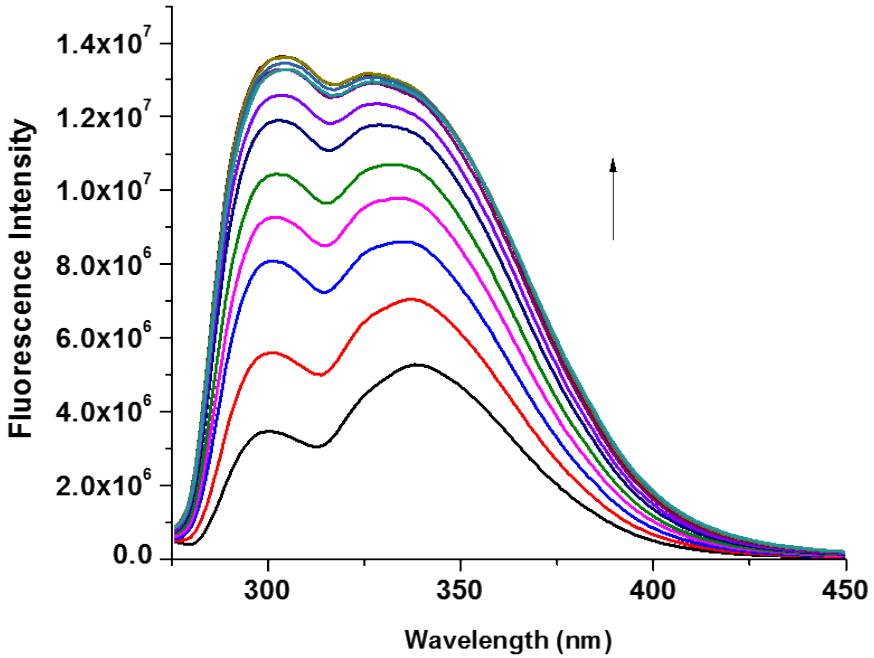


**Figure S7a**. Fluorescence titration spectra of receptor **2** (0.1 mM) in the presence of different concentrations of $Zn^{2+}$ (1 mM) (λex = 278 nm, λem = 341 nm, excitation and emission slit 5 nm) up to 10 µl (0.05 equiv.).

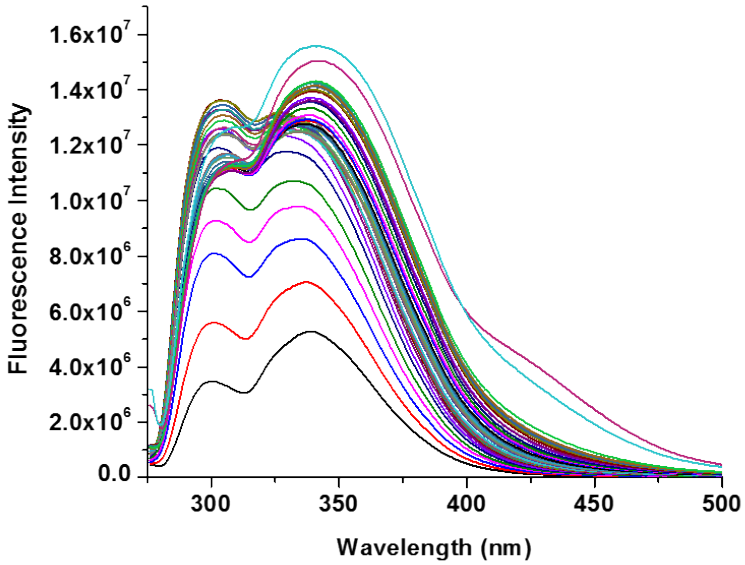


**Figure S7b**. Fluorescence titration spectra of receptor **2** (0.1 mM) in the presence of different concentrations of $Zn^{2+}$ (1 mM) (λex = 278 nm, λem = 341 nm, excitation and emission slit 5 nm) up to 400 µL (2 equiv.).

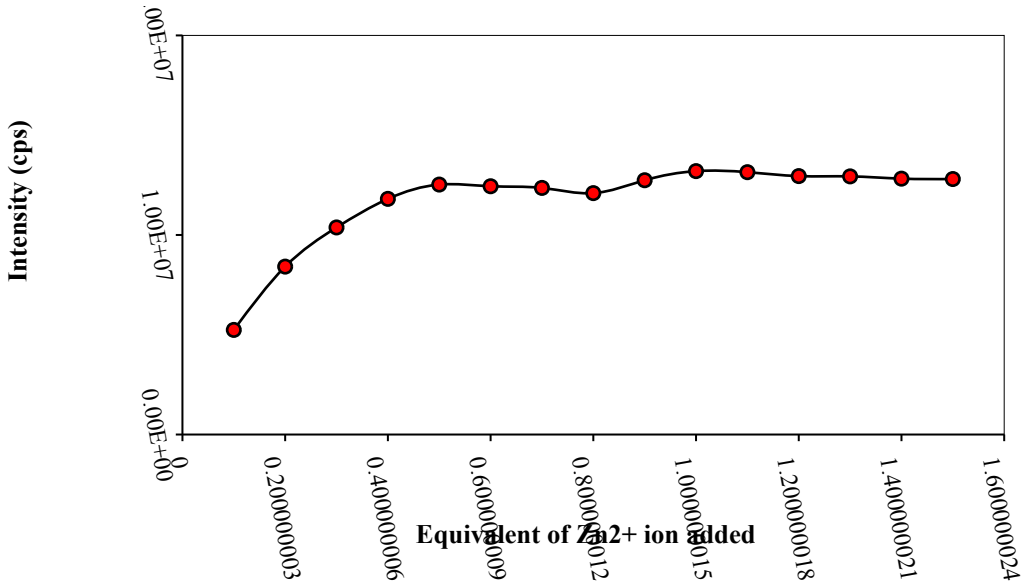


**Figure S7c**. Mole ratio plot (λem = 341 nm) illustrating the changing stoichiometry from 2:1 to 1:1.

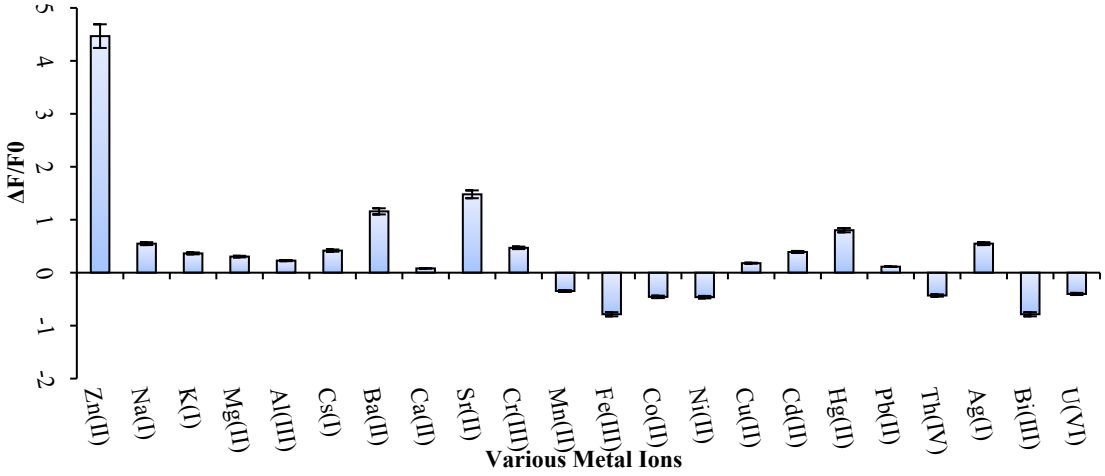


**Figure S8.** Fluorescence spectrometric response ($\Delta F = F - F_0$) of receptor **2** (0.1 mM) upon addition of 100 μL of respective cation salts (1 mM) in $CH_3CN/H_2O$.

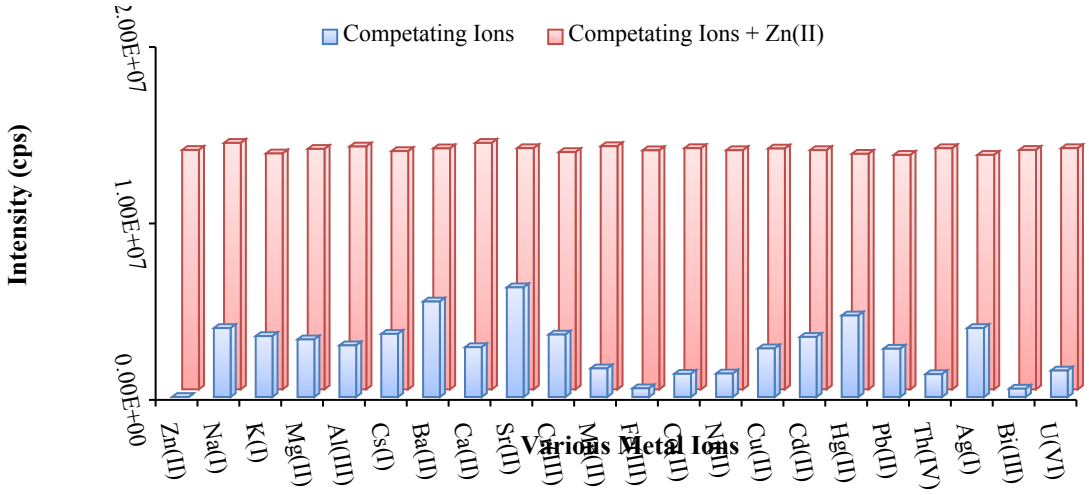


**Figure S9.** A fluorescence sensing of $Zn^{2+}$ ion (1 mM, 1equiv) by receptor **2** (0.1 mM) in the presence of other competing cations (1mM, 2 equiv.).

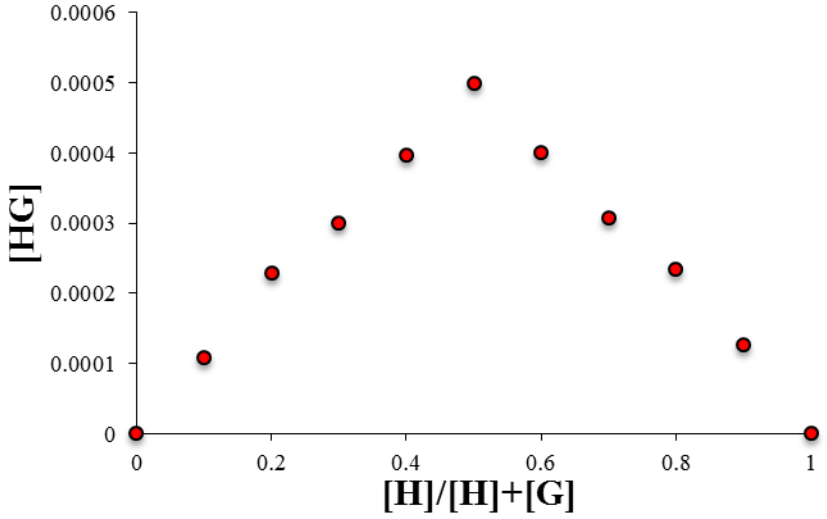


**Figure S10a.** Job's plot representing the stoichiometry of complex **2**.$Zn^{2+}$ (host : guest; 1:1).

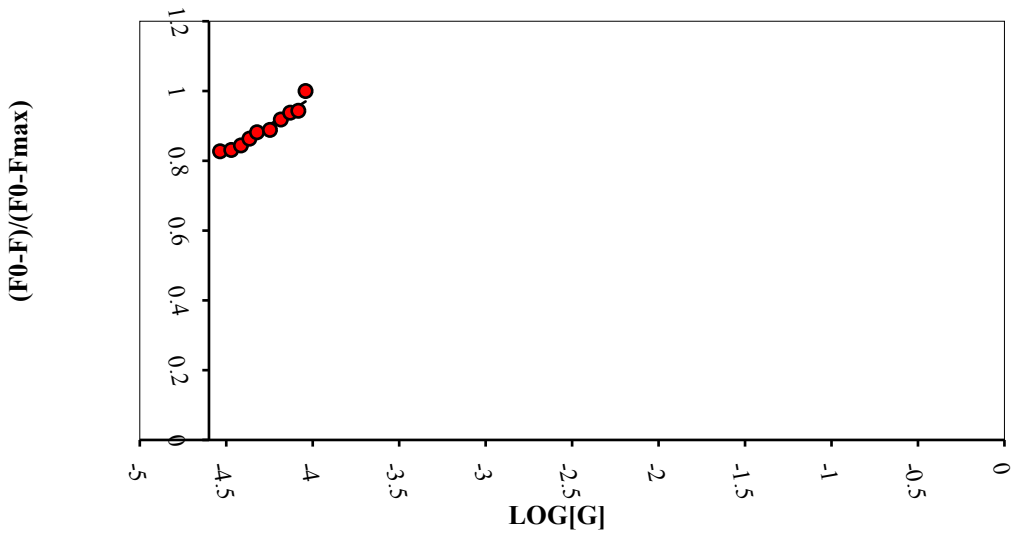


**Figure S10b.** Normalized plot obtained from fluorescence spectroscopy (λem = 341 nm).

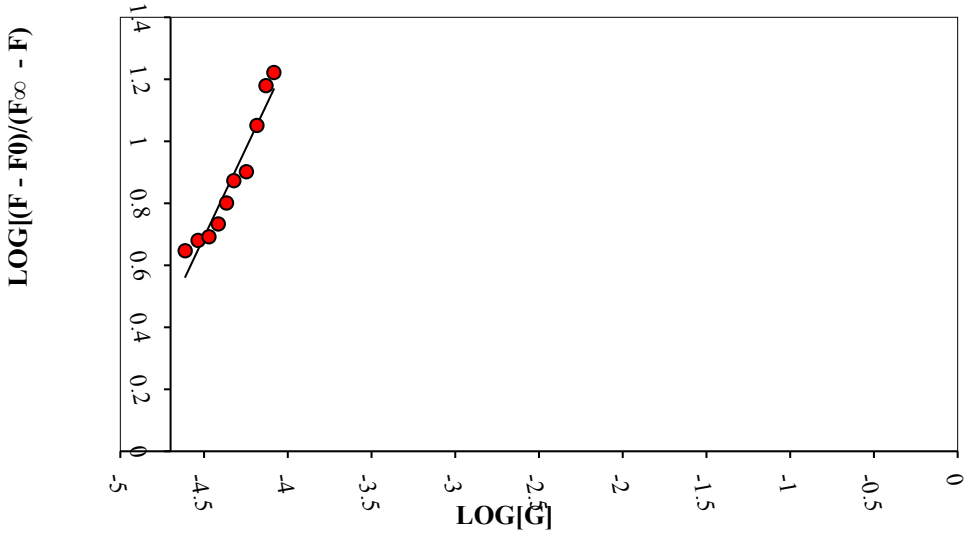


**Figure S10c.** Fluorescence intensity at 341nm of receptor **2** (0.1 mM) versus increasing concentration of Log[$Zn^{2+}$]. The fluorescence response fits to a Hill coefficient of 1.1446, which is in concordance with the 1:1 binding stoichiometry for the receptor **2**.$Zn^{2+}$ complex.

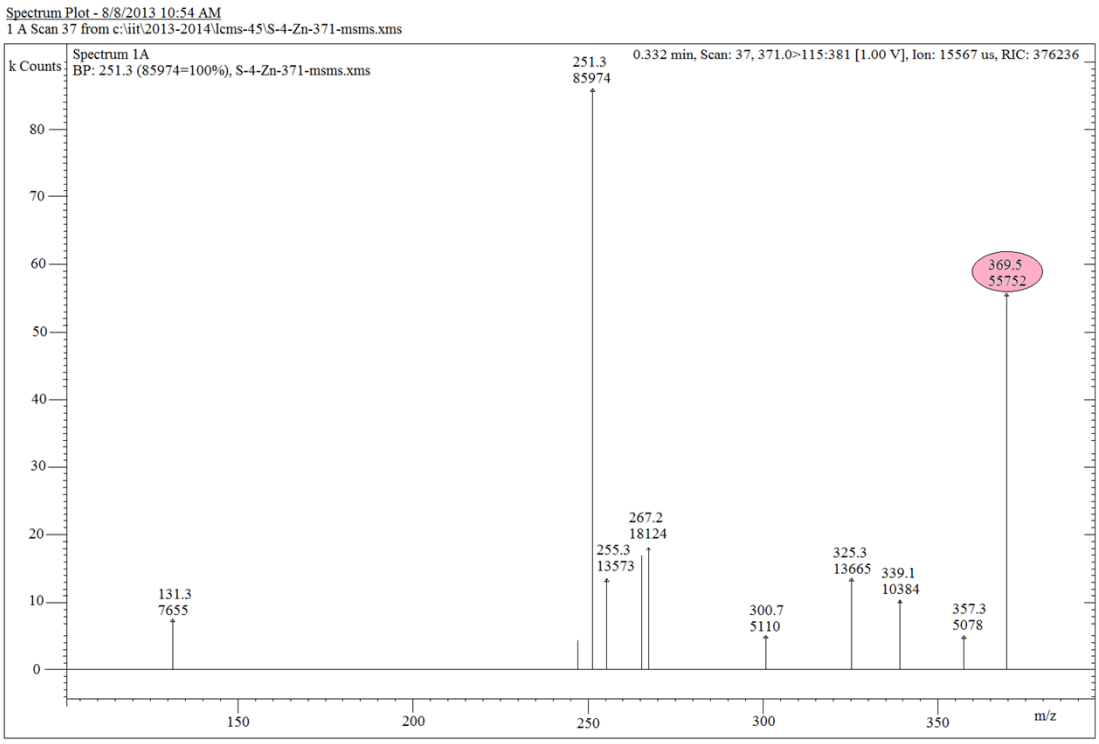


**Figure S11.** LC-MS spectra of **2.Zn$^{2+}$ complex (M+H$^{+}$)**

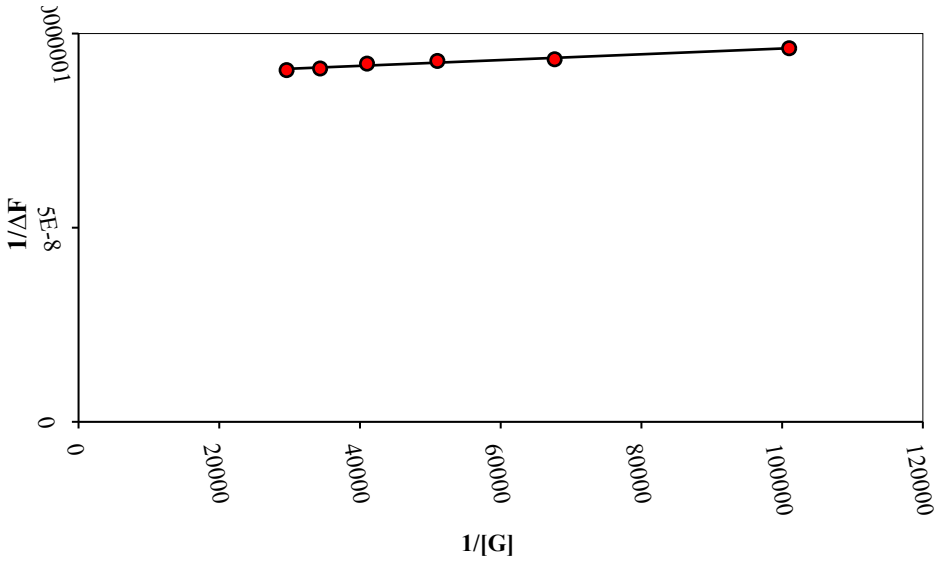


**Figure S12a.** A Benesi-Hildebrand methodology for receptor **2,** (1/Δ*F*) vs 1/[*G*], $K_a$ = $1.29 \times 10^6\ M^{-1}$.

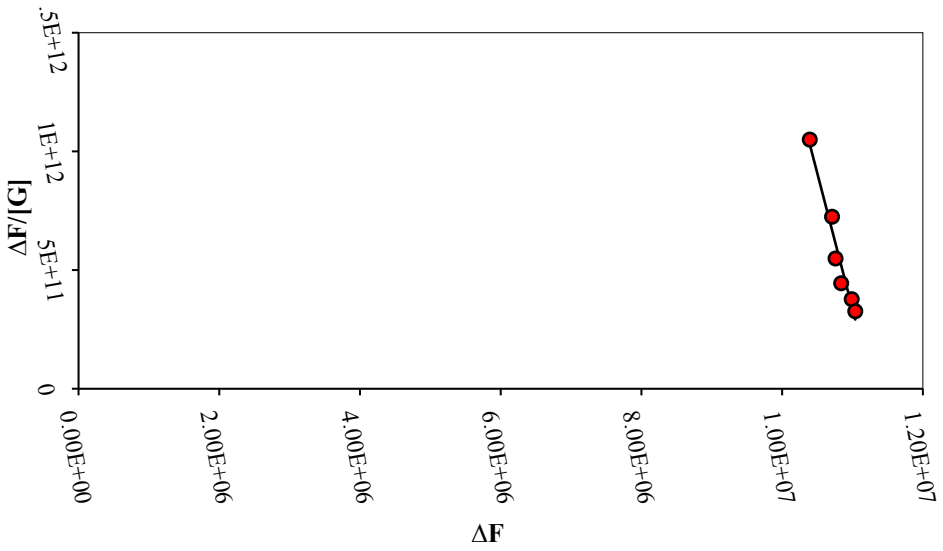


**Figure S12b.** A Scatchard methodology for receptor **2**, $\Delta F/[G]$ vs $\Delta F$, $K_a = 1.00 \times 10^6$ $M^{-1}$.

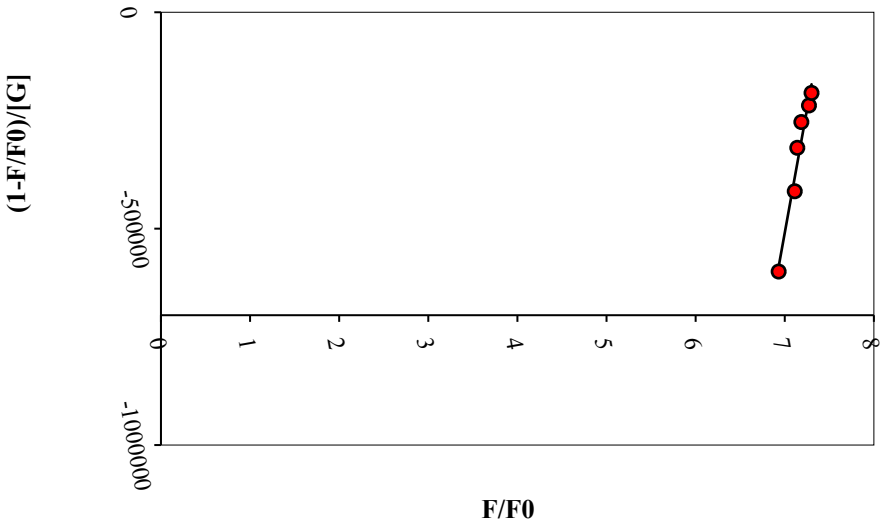


**Figure S12c.** Connor's fitting method for receptor **2,** $(1-F/F_0)/[G]$ vs $F/F_0$, $K_a = 1.94 \times 10^6$ $M^{-1}$

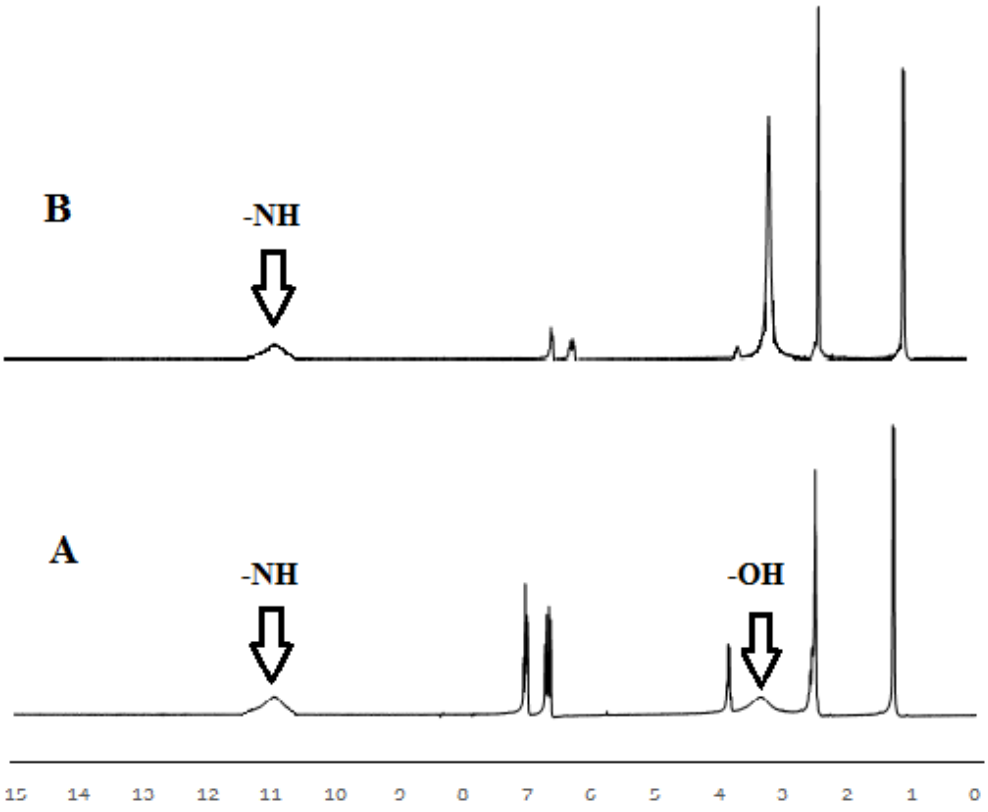


**Figure S13. $^{1}$H-NMR spectra (A) only receptor 2 (B) complex 3.**

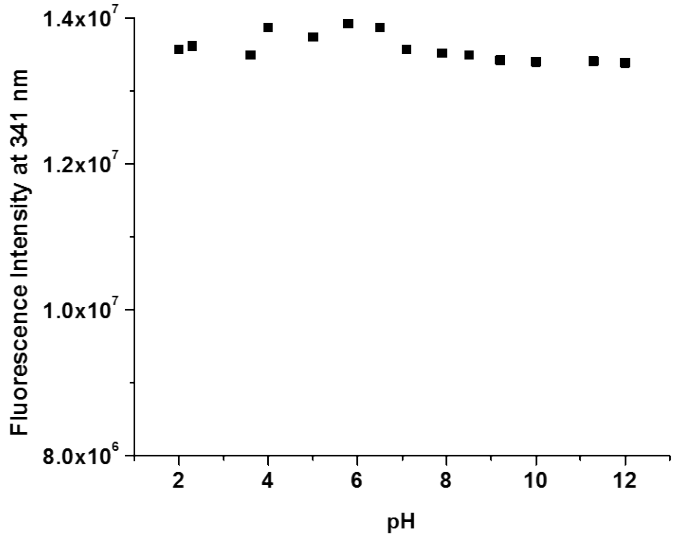


**Figure S14:** Change in fluorescence intensity of receptor **2** at 341 nm upon varying the pH of the solution.

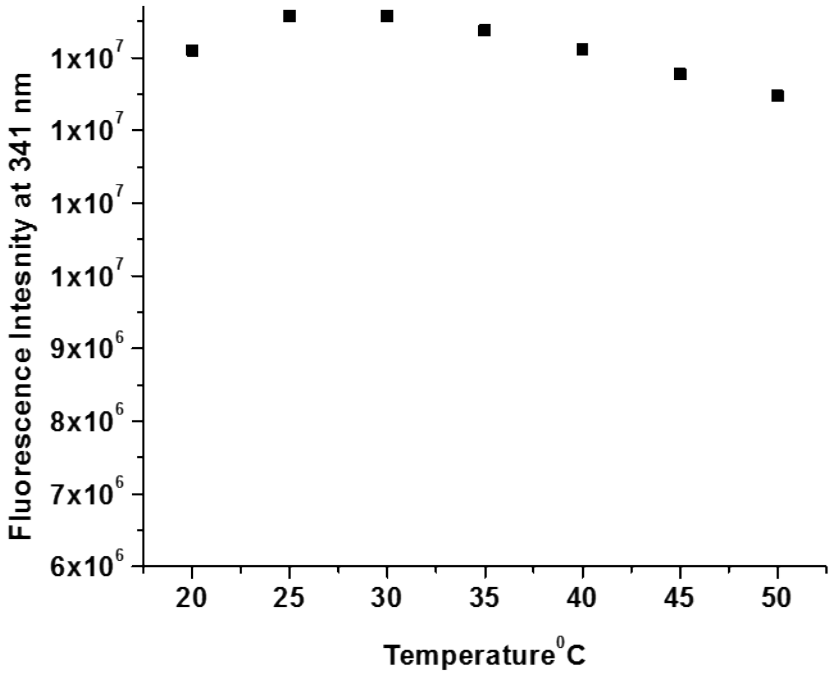


**Figure S15:** Change in fluorescence intensity of receptor **2** at 341 nm at various temperature.

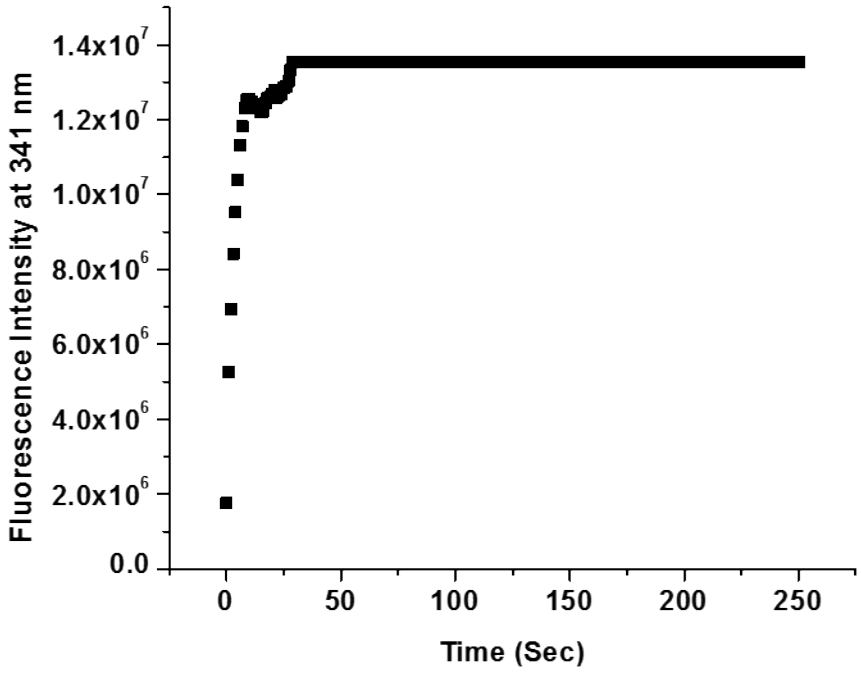


**Figure S16:** Fluorescence intensity of receptor **2** at 341 nm upon addition of $Zn^{2+}$ ion (1 mM) over time.

**Table S1:** Comparison of literature reports with present work.

| References | Detection Limit | Solvent |
|---|---|---|
| Zhou *et. al.,* (2012) | $2.2\times10^{-7}$ M | $CH_3CN$-$H_2O$ |
| Dong *et. al.,*(2014) | $1\times10^{-7}$ M | $CH_3CN$-Tris-HCl |
| Li *et. al.,* (2014) | $4.9\times10^{-8}$ M | $CH_3CN$-$H_2O$ |
| Kaur *et. al.,* (2014) | $1\times10^{-6}$ M | DMF-$H_2O$ |
| Sivaraman *et. al.,* (2012) | $1.5\times10^{-7}$ M | Phosphate buffer |
| Present work | $6.5\times10^{-7}$ M | $CH_3CN$-$H_2O$ |

**Table S2:** An optimized bond angles, dihedral angles, bond length and energy calculated at B3LYP/ LANL2DZ level.

| Parameter | Receptor **2** | **3** |
|---|---|---|
| **Dihedral angles (°)** | | |
| N25-C29-C30-N26 | 61.09 | 55.65 |
| C29-C30-N26-C24 | -135.57 | -158.35 |
| C5-C4-C23-N25 | 33.34 | 115.51 |
| O21-C3-C4-C23 | -0.50 | 6.07 |
| C27-C23-N25-C29 | -66.67 | -63.07 |
| C3-C4-C23-N25 | -147.43 | -68.10 |
| O22-C12-C11-C24 | -2.34 | 6.08 |
| C11-C24-N26-C30 | 157.50 | 169.33 |
| **Bond angles (°)** | | |
| C23-N25-C29 | 116.22 | 113.26 |
| C5-C4-C23 | 121.38 | 123.03 |
| C30-N26-C24 | 120.29 | 113.26 |
| N26-C24-C28 | 113.49 | 110.98 |
| N25-C29-C30 | 109.24 | 111.36 |
| **Bond Length (Å)** | | |
| N25-C29 | 1.46 | 1.52 |
| C30-N26 | 1.46 | 1.52 |
| C24-N26 | 1.47 | 1.54 |
| C23-N25 | 1.47 | 1.54 |
| C12-O22 | 1.39 | 1.46 |
| C3-O21 | 1.40 | 1.46 |
| O22-H45 | 0.97 | 0.97 |
| O21-H44 | 0.97 | 0.97 |
| N25-H42 | 1.01 | 1.02 |
| N26-H43 | 1.01 | 1.02 |
| C23-C27 | 1.54 | 1.53 |
| **Energy (a.u.)** | -960.28 | -1025.33 |